



Superior wear resistance of epoxy composite with highly dispersed graphene spheres

Hongyan Xia¹ · Jiajia Li¹ · Kai Wang¹ · Xinguang Hou¹ · Ting Yang¹ · Jiajun Hu¹ · Zhongqi Shi¹

Received: 8 February 2021 / Revised: 1 April 2021 / Accepted: 18 April 2021 / Published online: 29 April 2021
© The Author(s), under exclusive licence to Springer Nature Switzerland AG 2021

Abstract

Graphene has been proved to have an obvious superiority in suppression of the wear of polymers. However, the wide industrial application was suppressed by the bad graphene dispersion and complex preparation procedure. In this work, we employed carbon spheres coated with dispersed graphene (graphene spheres, g-AM) as filler to prepare the epoxy composites with direct mixing and curing. Comparing with neat epoxy and composites filled with calcined carbon spheres (CM, without graphene), the thermal and tribological properties of g-AM/EP composites were improved when the g-AM content was low. When chemical functionalization by grafting epoxy chain on the graphene (E-g-AM) was conducted, the total performance, especially the wear resistance, was remarkably improved even at high graphene content. The wear rate of E-g-AM/EP composites was reduced by 95% at 20 wt.% E-g-AM, compared to pure cured epoxy resin. This superior wear resistance was related to the synergistic effect of carbon spheres and graphene. Carbon spheres improved shore hardness and flexural strength, thus reducing the wear rate. The graphene had the high dispersion and good interface adhesion with epoxy, leading to the excellent lubricating effect and the improved mechanical and thermal performance of the composites.

Keywords Graphene · Hybrid · Thermosetting resin · Wear

1 Introduction

Thermosetting resins have excellent mechanical properties, corrosion, and chemical resistance, making them widely used as protecting materials in paint, building, automobile, aerospace, etc. [1–8]. However, the high friction coefficient and low wear resistance have always been the main reasons for limiting service life under some severe working conditions [9]. In order to improve the tribological properties, enormous efforts have been committed to introducing nano inorganic particles as fillers into polymer matrix, which can form a “high quality” tribofilm due to complex tribophysical and chemical actions. Because of the unique mechanical, tribological, and thermal properties of graphene and its derivative (graphene oxide, GO), recent investigations have paid much attention on graphene-filled polymer composites. Comparing with other nanofillers including SiO₂, TiO₂, Al₂O₃, Si₃N₄, and carbon nanotubes, graphene shows

an obvious superiority in suppression of the wear of polymers at very low contents [10, 11].

The typical wear mechanisms of neat thermosetting resin are adhesion wear and fatigue wear. After introducing graphene into the resin matrix, the enhancement in the tribological performance of graphene/resin composites can be explained based on stable lubricated tribolayer, excellent mechanical, and thermal properties. A robust protective transfer layer can be formed on the wear track during the friction testing, which offer a boundary lubrication role due to the easy inter-layer shearing [12–15]. Adding rigid graphene nanosheets into epoxy matrix could also improve the mechanical performance of hardness, which effectively reduce the penetration depth and restrain the adhesion wear during the sliding. Besides, graphene sheets with two-dimensional planar geometry were observed to bridge the micro-crack and debond/delaminate during fracture process, which would increase the fracture toughness value. It is worth noting that the strong interfacial adhesion between matrix and graphene nanofiller is very essential, which could transfer load effectively. Meanwhile strong graphene-epoxy adhesion/interlocking can increase the energy dissipating by matrix shear yielding and crack front pinning. Compared

✉ Hongyan Xia
hyxia0707@xjtu.edu.cn

¹ State Key Laboratory for Mechanical Behavior of Materials, Xi'an Jiaotong University, Xi'an 710049, China

to the pristine polymer, the existence of graphene sheets increased the thermal conductivity and glass transition temperature of the composite, preventing polymer chains from oxidation and decomposition at high temperature during serious friction procedure [16–21].

Facile and low-cost preparation procedure is very important for industrial application of graphene-filled polymer composite. Graphene is typically produced using mechanical and chemical exfoliation, chemical vapor deposition (CVD), and thermal deposition from solid sources. The mechanical and chemical exfoliation are effective for the high-yield and low-cost production of graphene or graphene oxide from bulk graphite. Thermal deposition from solid sources and CVD methods from gas sources have been used to synthesize large size graphene sheets on silicon, copper, or other metal substrates [22–28]. However, comparing with other nano inorganic particles, these methods are still costly and not facile which cannot make graphene a potential candidate for extensive usage as the filler in polymer composites. Moreover, graphene dispersion is widely recognized as a challenge in polymer nanocomposites fabrication. And the inferior dispersion of graphene can cause cracks, pores, and pin holes in the composite, which greatly worsen the friction and wear performance. At present, three main methods of manufacturing graphene-polymer composites are mainly focused: in-situ polymerization, solution compounding, and melt blending [29–34]. However, these methods are still complex and have difficulty in obtaining high graphene dispersion.

In our previous paper, highly dispersed graphene which coated on the carbon spheres (graphene spheres, g-AM) was prepared [35]. This kind of graphene structure maintains strong dispersion condition and can mix with polymers directly. In order to investigate the application potential as filler of polymer-based composite, we employed the graphene spheres as filler to prepare epoxy resin-based composite in this work. The microstructure, thermal, and mechanical performance were measured. Based on these results, the friction and wear behavior were carefully tested and analyzed.

2 Experimental

2.1 Materials and preparation

Epoxy resin (EPON 862) based on diglycidyl ether of bisphenol-F (DGEBA), with an epoxy equivalent weight of 165–173 g/eq, and curing agent diethyltoluene diamine (DETDA) with an amine equivalent weight of 113 were provided by Hexion Inc., China.

Three kinds of carbon fillers were used to prepare the epoxy-based composites in this work: g-AM spheres, epoxy chain-modified g-AM (named as E-g-AM), and calcined

MCMB (CM). g-AM spheres were gotten by chemical activation of MCMB with KOH, and the details can be seen in the literature [35]. In order to strengthen the interfacial interaction of graphene and epoxy matrix, chemical functionalization by grafting epoxy chain on the graphene spheres was also conducted to obtain E-g-AM, using similar procedure as the literatures [36–37]. The details of grafting epoxy chain on graphene spheres were as follows: EPON 862 epoxy resin was dissolved in acetone by vigorous stirring. Then, g-AM was added, with the weight ratio 1.0% to epoxy, and ultrasonic dispersed for 30 min. Catalyst of NaOH aqueous solution (weight of NaOH was 0.25, 0.5, 1, and 10 wt.% to epoxy) was added into the mixed solution to catalyze the reaction. After the reaction coupled with magnetic stirring at 70 °C for 5 h, the reactants were washed with acetone and deionized water through filtration-washing method and finally dried in an oven to obtain epoxy chain grafted g-AM (named as 0.25E-g-AM, 0.50E-g-AM, 1.00E-g-AM, and 10.00E-g-AM based on the weight of NaOH to epoxy). Based on the amount of grafted epoxy, 1.00E-g-AM was finally chosen as the filler of composites. For comparison purpose, calcined MCMB without any graphene was also used as the filler, which was obtained by heat treatment at 1000 °C for 1 h in nitrogen atmosphere.

The preparation of the composite was facile: carbon filler (weight percentage of 0, 3, 5.6, 10, and 20% in the composite) was directly mixed with pre-heated epoxy resin by mechanical stirring for 60 min, during which a few acetone was added to decrease the viscosity. The mixture was subsequently dried in oven to remove the acetone completely. Afterwards, the curing agent was added into the above mixture with mass ratio of 66 (DETDA) to 100 (DGEBA) and mechanically stirred and degassed for another 20 min with a vacuum pump to eliminate air bubbles. Then, the as-prepared mixture was transferred onto an open mold and cured at 60 °C for 24 h and then at 150 °C for 6 h in air oven.

2.2 Tribological tests

Tribological tests were carried out on a reciprocating ball-on-flat contact tribometer (LFT-1, Zhongke Kaihua, Lanzhou, China) in air at room temperature. The flat of specimen was fixed on the base of the tribometer, which moved back and forth with a constant stroke $\Delta\chi$ and a frequency of ν . The counterpart ball, bearing steel GCr15 with a diameter of 5 mm, was mounted on top of horizontal flat specimen and loaded with normal force F_N . In this work, the normal load F_N was fixed at 20 N, and the stroke length $\Delta\chi$ was 5 mm with a frequency ν of 500 rpm, meaning that the sliding linear speed was 0.083 m/s. The sliding time for each test was normally 20 min. Prior to the test, all the contact surfaces were cleaned with ethanol. For each sample, at least

three trials were conducted to ensure repeatability of test data.

The value of friction coefficient was obtained by the friction stress divided by normal force, and the friction stress was obtained by a force transducer and recorded in the computer. The wear rate W was calculated by $W = S/l / (L \cdot F_N)$, where S was the sectional worn area measured by a non-contact 3D surface profiler; l was the stroke amplitude, 5 mm; and L is the total sliding distance in 20 min.

2.3 Characterization

The morphology of carbon fillers and fracture cross-sections of composites were investigated by the scanning electron microscope (SEM, Quanta 600FEG, USA). Fourier transform infrared (FTIR) spectrum between 600 and 3000 cm^{-1} for surface-functionalized g-AM was obtained using an IR Prestige-21, in which the epoxy was cured bulk sample and g-AM and E-g-AM were powders. In order to measure the grafted epoxy content and characterize the thermal stability of the composites, the thermogravimetric (TG) curves of the E-g-AM and composites were measured by high-temperature thermal analyzer (SDT Q600, USA), with heating rate of 10 $^{\circ}\text{C}/\text{min}$ and a nitrogen flow of 100 ml/min in N_2 atmosphere. The thermal diffusivity of samples was measured using laser thermal conductivity instrument (LFA-467, NETZSCH), with sample size of 12.7 mm in diameter and 1 mm in thickness. Furthermore, the thermal conductivity was obtained based on the relationship $\lambda = \rho \alpha C_p$, where

λ was the thermal conductivity, ρ the bulk density, α the thermal diffusivity, and C_p the specific heat capacity. Digital shore hardness test (LX-D, ASTM D2240) was used to measure the hardness. The three-point bending strength was measured with a 16 mm span at a cross head speed of 0.5 mm/min. After the wear test, the worn surface and longitudinal section were characterized using a SEM and 3D surface profiler (VK-9700, Keyence, Osaka, Japan). The structure and composition of the worn surface was characterized using X-ray photoelectron spectroscopy (XPS; Axis Ultra DLD, Kratos, UK) and the laser Raman spectrophotometer (HR800, Horiba, France), with 633 nm laser wavelength excitation and 17 mW laser power.

3 Results and discussion

3.1 Characterization of carbon fillers

The CM filler was rather coarse, and no graphene existed on the surface, as seen in Fig. 1a. By comparison with CM, the g-AM spheres had graphene flowers on the surface, with strong resistance to be aggregated, as seen in Fig. 1b. For the epoxy functionalized g-AM, the high magnification morphologies of 1.00E-g-AM and 10.00E-g-AM (1.0 and 10.0 wt.% NaOH to epoxy) are shown in Fig. 1c, d. The thickness of graphene increased clearly when the mass ratio of catalyst NaOH to epoxy changed from 1 to 10, which meant that more epoxy was probably grafted on the surface of graphene.

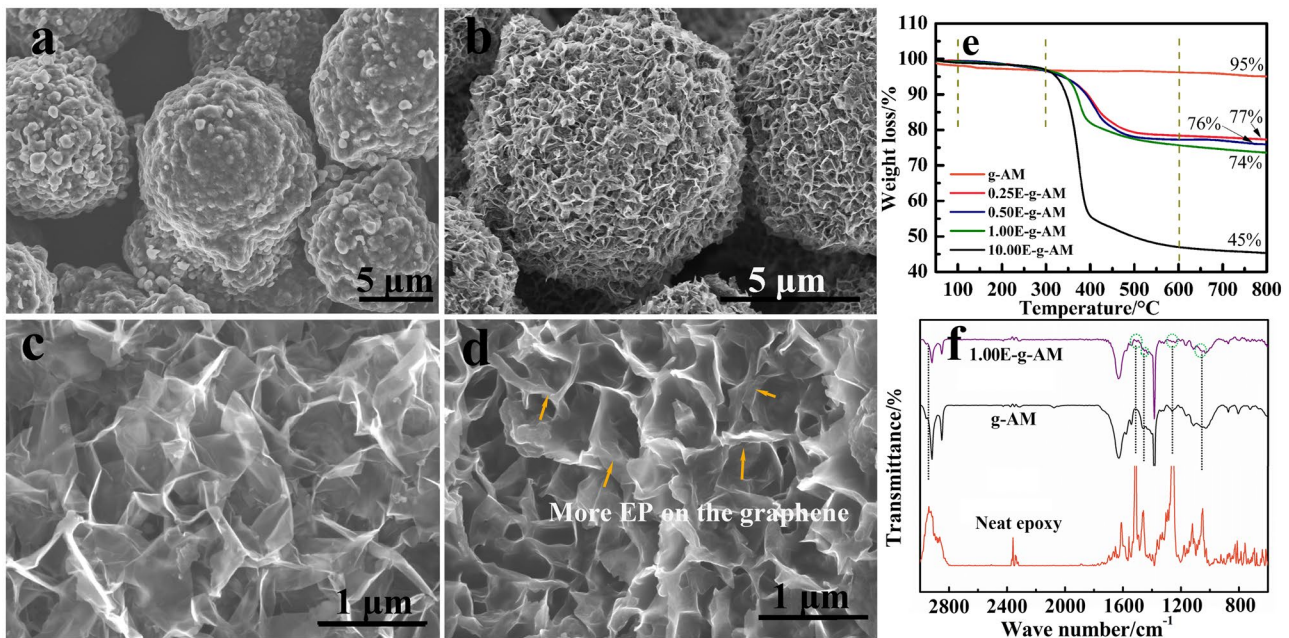


Fig. 1 SEM images of **a** calcined MCMB; **b** g-AM; **c** epoxy grafted 1.00E-g-AM; **d** epoxy grafted 10.00E-g-AM; **e** TG curves of the epoxy grafted g-AM with different catalyst content; **f** FTIR spectrum of g-AM, 1.00E-g-AM, and pure epoxy resin EPON 862

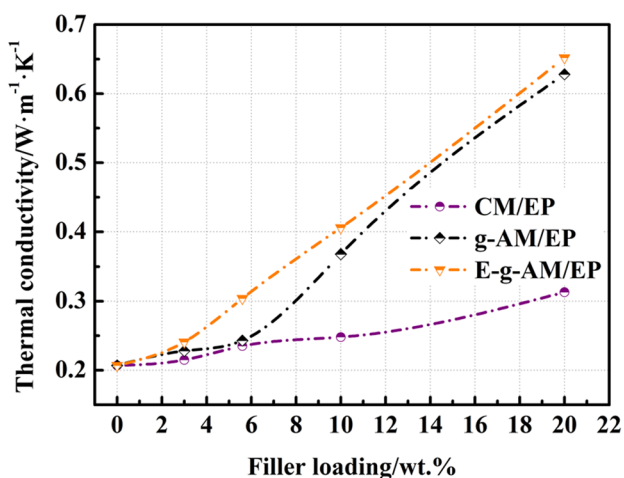


Fig. 2 Thermal conductivity of the three kinds of composites with different filler content at room temperature

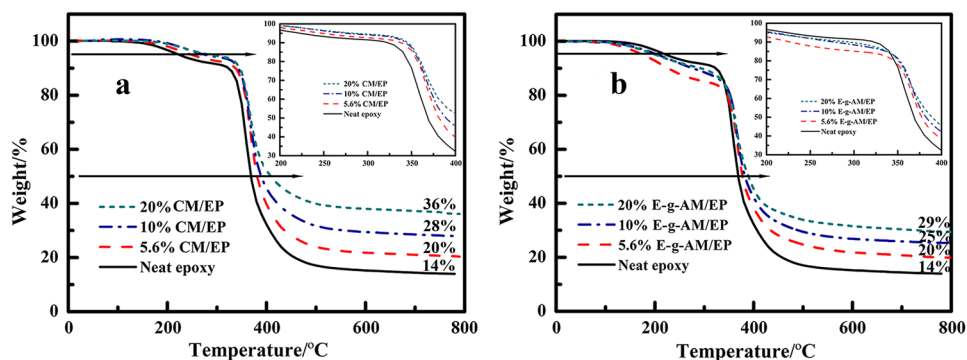
In order to calculate the amount of epoxy chain grafted on the graphene, the thermogravimetric curves of E-g-AM were tested and given in Fig. 1e. The results show that there were mainly two thermal weight loss stages, appeared separately at 100–300 °C and 300–600 °C. The former mild weight loss was due to the decomposition of surface oxygen-containing functional groups with the increase of temperature. The latter sharp weight loss above 300 °C was resulted from the degradation of the grafted epoxy [36]. On the base of the residue at 800 °C, the weight of grafted epoxy was about 26 and 55 wt.% when the mass ratio of NaOH to epoxy was about 1 and 10, respectively. Figure 1f shows the FTIR spectra of epoxy grafted g-AM, ungrafted g-AM, and epoxy resin, in which the mass ratio of NaOH to epoxy is 1.0 for the epoxy grafted g-AM (1.00E-g-AM). Compared with g-AM, the 1.00E-g-AM had new characteristic absorption peaks at 1503, 1451, 1259, and 1056 cm^{-1} , which corresponded to the benzene ring and ether groups of epoxy, indicating that epoxy chains were successfully grafted on the graphene [36].

3.2 Thermal properties

Figure 2 shows the thermal conductivity of the three kinds of composites with a series of volume fraction at room temperature. For the neat epoxy, the measured thermal conductivity of epoxy resin was about 0.21 W/m·K. After adding carbon filler CM, g-AM, and E-g-AM, the enhancement on thermal conductivity was seen for all the measured composites. Compared to CM/EP, the thermal conductivity of g-AM/EP and E-g-AM/EP composites was remarkably increased when the content was above 5.6 wt.%. For E-g-AM/EP sample, it is 0.65 W/m·K when filled with 20 wt.% E-g-AM, enhanced by 210% compared to the pure cured epoxy. Although the graphene prepared from activation had lots of defects and oxygen containing groups, it is still helpful to improve the thermal conductivity of the composites.

Figure 3 shows the thermogravimetric analysis curves of CM/EP and E-g-AM/EP, which are used to characterize the thermal stability of the epoxy composites. The pure epoxy resin began to decompose at about 150 °C and became serious at stage of 320–500 °C, which corresponded to the thermal decomposition of aromatic groups of the epoxy network and aliphatic amine curing agent. For the epoxy composites, the main degradation procedure occurred between 320 and 500 °C, similar to pure epoxy. From the insert of high magnification image at 200–400 °C, the weight loss rate of the epoxy composites, especially CM/EP composite, was slower than that of the pure epoxy resin. With the increase of the mass fraction of the fillers, 30% thermal weight loss temperature (T_{30}) increased from 355 °C for neat epoxy to 365, 367, and 370 °C for 5.6, 10, and 20%CM/EP composites and 360, 363, and 363 °C for 5.6, 10, and 20%E-g-AM/EP composites. It means the thermal degradation temperature of the composites went up slightly, which indicated that the thermal stability of the composites was improved with the increase of the filler content [38]. Based on the remained weight at 800 °C, the mass loss percentage of the epoxy in the CM/EP was decreased but increased in the E-g-AM/EP compared to neat epoxy. The possible reason is that the

Fig. 3 The thermogravimetric analysis curves of **a** CM/EP and **b** E-g-AM/EP samples. The inserts were the high magnification images from 200 to 400 °C



calcined carbon can improve the intermolecular crosslink and prevent polymer chains from the decomposition at high temperature, but the E-g-AM, which had oxygen containing groups, may mildly accelerate the oxidation, and the surface grafted epoxy also can increase the weight loss.

3.3 Mechanical properties

Figure 4 presents the flexural strength and shore hardness of the composites. In general, the change tendency of strength and hardness was increased first and then decreased with increasing the filler content. Among the three carbon fillers, the g-AM filler had mildly positive effect only at low content and would remarkably reduce the flexural strength and shore hardness with increasing the fillers content over 5.6 wt.%. On the contrary, the E-g-AM with surface modification had the best effect on the improvement of mechanical properties of composites. The flexural strength and shore hardness of neat epoxy was 96 MPa and 85 HD, respectively. After the introduction of E-g-AM fillers at appropriate mass percentage, the strength and hardness reached up to the highest values of 120 MPa (increased by 25%) and 87 HD. Figure 5 shows the cross-sectional SEM images of pure cured epoxy and carbon-filled composite after bending fracture. The cross-section of the pure epoxy resin was flat and smooth and revealed brittleness destruction characteristic. Compared with the pure epoxy resin, the cross-section of the composites presented rough and uneven surface, and the number of river branches was significantly increased. For g-AM/EP, graphene was uniformly coated on the surface of carbon microspheres, without peeling off and agglomeration. However, the graphene layers with large surface area were not well interface bonded with epoxy and made much coarser fracture section than those of CM/EP and E-g-AM/EP. This weak interface bonding was not beneficial to inhibit crack propagation and increase energy dissipating by crack front pinning and graphene bridging, which resulted in the sharp decrease in the mechanical performance at high g-AM content. After surface treatment of graphene with epoxy, the fracture surface became smoother even in the pits left by

the detached carbon spheres, which proved that the interfacial interaction became stronger. The reason should be that the epoxy was successfully grafted onto graphene via the reaction between the epoxide groups in epoxy and the carboxy groups on graphene with the assistance of NaOH catalyst. Since each epoxy chain had two terminated epoxide groups, one epoxy chain connected to graphene, the other one participated in the subsequent curing reaction [36]. This strong interface bonding improved the ability to hinder crack propagation and energy dissipating under loading condition, leading to the increased hardness and strength.

4 Friction and wear

In order to explore the influence of graphene and interface interaction on the friction and wear behavior of the composites, dry sliding test was conducted by a reciprocating ball-on-disk configuration tribotester under a load of 20 N.

Figure 6a, b shows the change of friction coefficient of CM/EP as function of sliding time and average values for composites with different filler content. After the initial 4–6 min running-in stage, the curve of friction coefficient versus sliding time for neat epoxy showed a steady trend gradually, while it was still unstable for CM/EP composite. Neat epoxy presented a high friction coefficient with the average value of about 0.72 at stable stage. Compared to neat epoxy, there was no remarkable reduction in friction coefficient and lubrication effect with the introduction of CM into the CM/EP composite. This means the calcined MCMB should have poor lubrication effect on the friction behavior for the composite, even at high weight content, which fits well with other report [39].

Figure 6c, d shows the curve of friction coefficient versus sliding time and average friction coefficient values for g-AM/EP composite. Compared with CM, graphene coated on the MCMB can reduce the friction coefficient of epoxy composite significantly. When the filling amount reaches 20 wt.%, the friction coefficient decreased to about 0.48, which dropped by 34% compared to pure epoxy resin. After

Fig. 4 a Flexural strength and b shore hardness of the composites

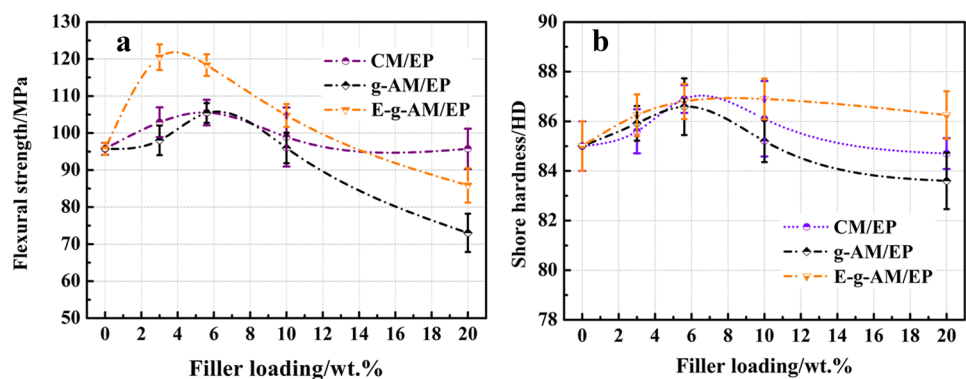
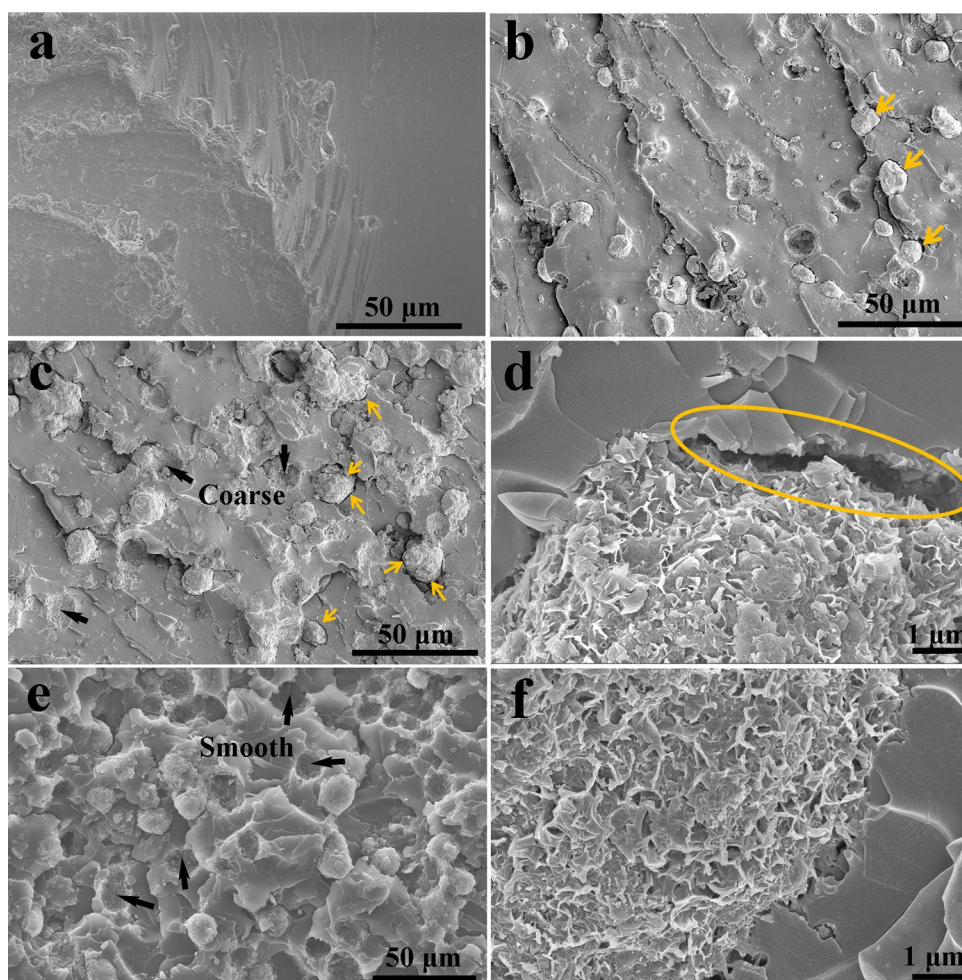


Fig. 5 Cross-sectional SEM images of cured samples: **a** pure epoxy; **b** CM/EP with 10 wt.% CM filler; **c** and **d** g-AM/EP with 10 wt.% g-AM filler; **e** and **f** E-g-AM/EP with 10 wt.% E-g-AM filler



strengthening the interface bonding between graphene and epoxy, the friction coefficient further dropped to 0.40 (dropped by 45%) (Figs. 6e, f). Figure 7 reveals the comparison of friction coefficient change tendency of CM/EP and E-g-AM/EP composites at the later stage under high magnification. The curve showed the lubrication characteristic for E-g-AM/EP, which proved the better lubrication effect of graphene.

Figure 8 presents the wear rate of the composites with different filler content, featuring somewhat different trend with the friction coefficient. The wear rate of neat EP was as high as $2.36 \times 10^{-4} \text{ mm}^3 \cdot \text{N}^{-1} \cdot \text{m}^{-1}$ and significantly was reduced by the introduction of carbon fillers. The highest reduction of wear rate reached up to 37, 63, and 95% for CM/EP, g-AM/EP, and E-g-AM/EP, respectively. This reduction extent in wear rate was much higher than that in friction coefficient, which revealed that graphene had more positive influence toward the suppression of wear than the reduction in friction coefficient in the epoxy-based composites. Besides, for g-AM/EP, it was seen that the wear rate at 20 wt.% filler was increased again, due to the more defects induced by the weak interface bonding between graphene

and epoxy matrix. As a result, surface modification of graphene spheres was extremely essential for the preparation of the composite in our work.

Observation of the worn surface of neat epoxy by 3D surface profiler (in Fig. 9a) showed the large peeling regions, pits, and serious crack propagation perpendicular to sliding direction, indicating that the neat epoxy suffered from a serious adhesion damage under reciprocating sliding by the steel ball counterpart. Large cracks with lots of epoxy debris accumulated around the wear track were visible by the naked eyes. The SEM image in Fig. 10a exhibited highly loose structure with large holes and cracks on the worn surface. It was further discovered that the inner wall of some holes was smooth, which implied that the worn surface temperature was very high and the thermal decomposition of epoxy matrix happened. This evidence indicated the serious friction and wear happened for neat epoxy, which produced a large quantity of heat during friction process.

As for CM/EP composite in Fig. 9b, adhesion wear was significantly weakened. However, although the amounts of cracks and pits were much lesser than that of neat epoxy, the worn surface still had lots of rough regions (black regions).

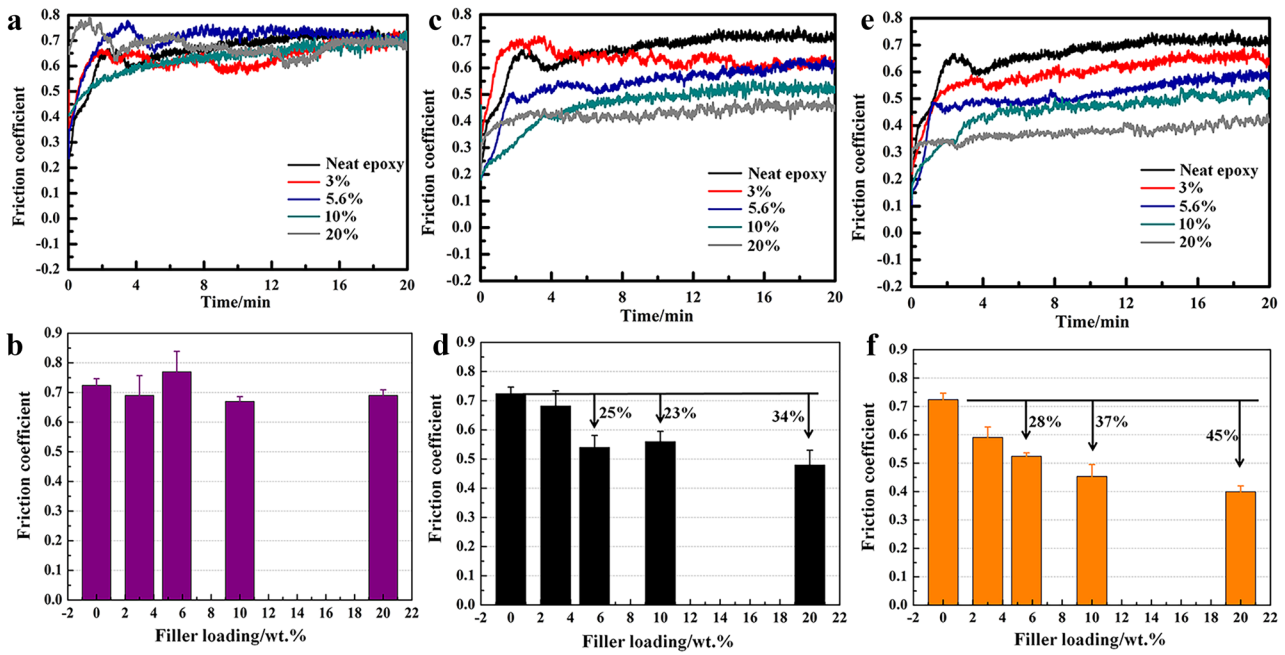


Fig. 6 The curves of friction coefficient versus sliding time and average friction coefficient value at steady stage: **a** and **b** CM/EP; **c** and **d** g-AM/EP; **e** and **f** E-g-AM/EP

According to the SEM investigation in Fig. 10b, the rough regions were plowing pits, which can cause unstable friction behavior for CM/EP composite. With the addition of graphene into the composites, the worn surfaces of g-AM/EP became much smoother relative to the pure epoxy and CM/EP composite, as seen in Figs. 9c and 10c, yet there were a number of long and thin cracks generated and propagated under the reciprocating pressure, which should be resulted from the weak interface bonding between graphene and epoxy resin. Strengthening the interface bonding by

surface modification prevented the occurrence of cracks, which made the worn area and crack length significantly decreased, as shown in Figs. 9d and 10d. The wear area of E-g-AM/EP measured by 3D surface profiler was 0.0046 mm², reduced by 95% and 92% compared to pure EP and CM/EP composite, respectively. Figure 10e, f also shows the element-mapping results of worn scar of the CM/EP and g-AM/EP composites. There was no Fe element detected. The element C distribution of CM/EP composite was uneven, which revealed that it was difficult to form the stable and uniform protective transfer layer on the worn surface. For E-g-AM/EP composite, the element C distribution was uniform, which meant that graphene containing carbon filler was located uniformly on the worn scar.

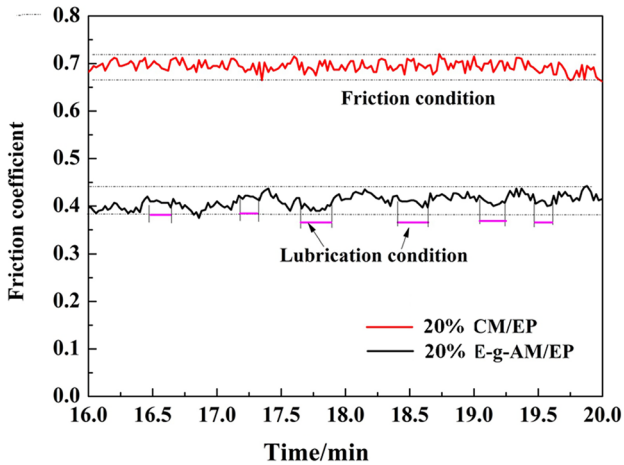


Fig. 7 Friction coefficient versus sliding time of 20%CM/EP and 20%E-g-AM/EP at the later stage under high magnification

Observation on the longitudinal sections of the three specimens (neat epoxy, 20%CM/EP, and 20%E-g-AM/EP) displayed the microstructure features of the subsurface below the worn surface, as shown in Fig. 11a–c. It can be seen that a third-body tribolayer with thickness of about 44, 29, and 4 μm located on the top of substrates of the above three samples. The tribolayer of neat epoxy was plastic deformation region. And after adding carbon fillers, the tribolayers of the composites were mechanically mixed layer (MML) from wear debris, which were subjected to complicated process of fragmentation, mixing, oxidation, and compacting under normal load and frictional force to form MML [40]. The MML was mainly decided by the microstructural features of the original base materials and could have a strong influence on the friction performance

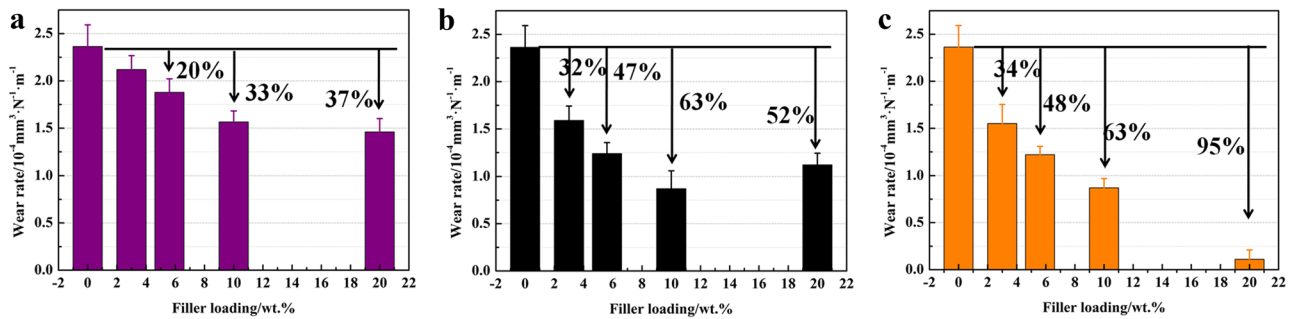


Fig. 8 Wear rate of the composites with different filler content: **a** CM/EP; **b** g-AM/EP; **c** E-g-AM/EP

and wear resistance. The thin and smooth MML can be stable located on the surface of the base, which contributed to the increase of local contact area, further reducing the contact pressure and friction force. On the contrary, the thick and uneven MML was unstable and can easily be peeled out from worn surface, which accelerated the generation of high and unstable friction coefficient and high wear rate. These observations of longitudinal sections, once again, demonstrated the difference in the friction and wear behavior among the three kinds of composites.

To further understand the composition of the wear track, XPS spectrum of worn surfaces is given in Fig. 11d, e. The relative peak area of C–OH at 285.1 eV was larger than that of C–O–C at 286.5 eV for the E-g-AM/EP composite but conversely for CM/EP. It is indicated that the oxidation of epoxy matrix of CM/EP was more serious than E-g-AM, which can worsen the friction and wear of the composite. Micro-Raman spectroscopy of worn surfaces was done to investigate the microstructural changes after reciprocating

sliding against the counterpart of stainless-steel ball. In Fig. 11f, the Raman spectra of the CM/EP and E-g-AM composites before and after wear are displayed. For the E-g-AM composite, typical peaks at 1576 and 2697 cm^{-1} , referred to the graphene *G* and *2D* peak, can be clearly seen before wear. Also, the spectrum taken from the pristine composite showed three strong Raman signals at about 1605, 2918, and 3060 cm^{-1} , which can be assigned to the phenyl ring, phenyl-hydrogen, and methyl stretches of the DGEBF molecule [41]. After the wear test, the *D* peak at 1344 cm^{-1} to disordered carbon appeared, and signals to epoxy and graphene became weak and broadened. This change indicated that tribophysical and chemical reactions happened on the composite surface, and there was graphene that existed on the worn scar although the disorder was increased. For the CM/EP composite, the signal to carbon was weak, and peaks at 2918 and 3060 cm^{-1} to epoxy nearly vanished after wear. It means that network molecule structure of epoxy in the CM/EP was more seriously destroyed than E-g-AM.

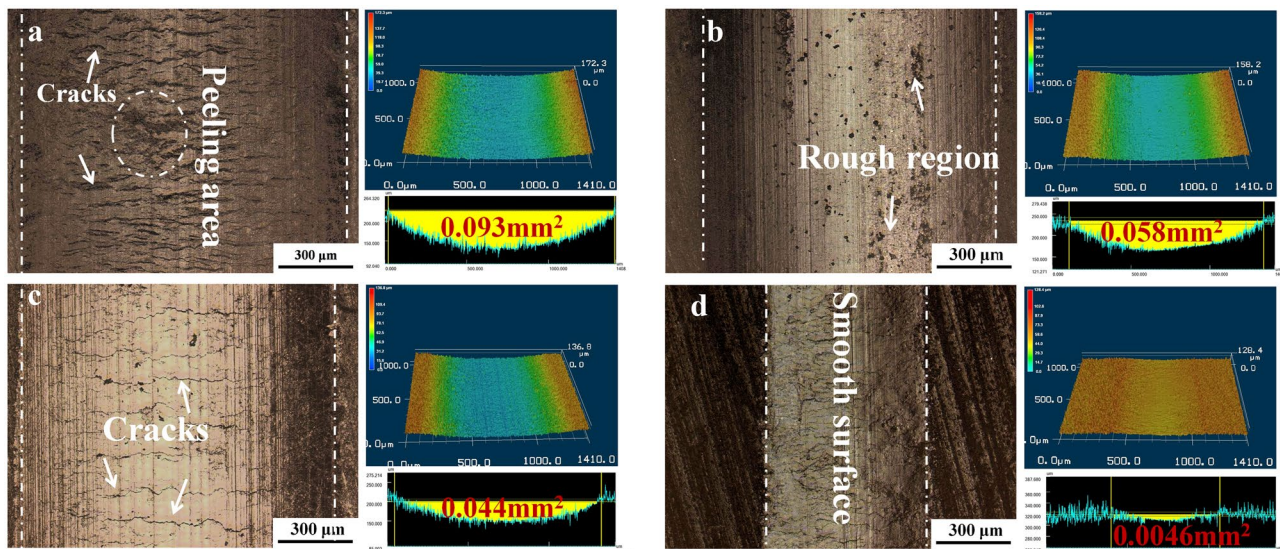


Fig. 9 Optical topographies of worn surfaces of composites measured by 3D surface profiler: **a** neat epoxy; **b** 20%CM/EP; **c** 20%g-AM/EP; **d** 20%E-g-AM/EP

Fig. 10 SEM images of worn surfaces of composites: **a** pure epoxy; **b** 20%CM/EP; **c** 20%g-AM/EP; **d** 20%E-g-AM/EP; **e** C element-mapping of **e** 20%CM/EP and **f** 20%E-g-AM/EP

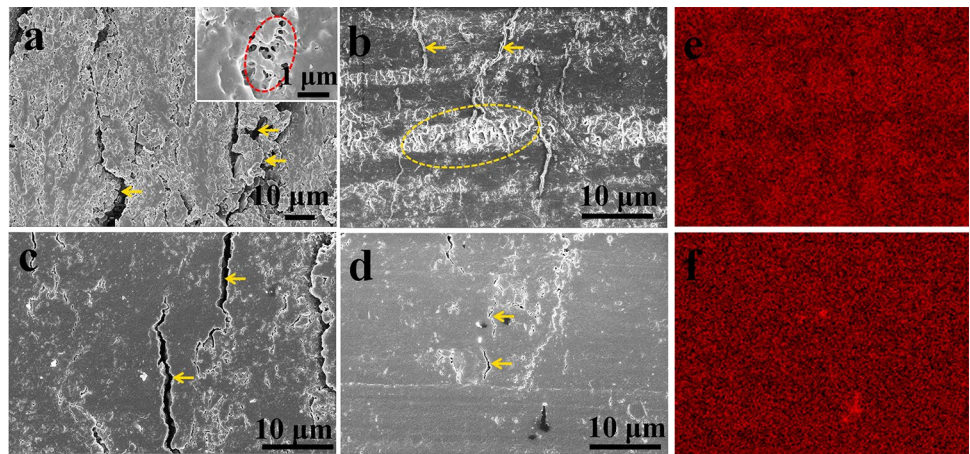


Figure 12 further elaborates the friction mechanism of the neat EP and epoxy composites. For neat EP with low hardness and strength, under dry sliding conditions, cracks were easily generated, and obvious adhesive wear occurred. The substantial heat generated during the friction process would accelerate the thermal decomposition of epoxy matrix, which can seriously worsen the friction and wear process. The very rough surface made no MML formation on the worn surface, as seen in Fig. 12a. CM/EP had improved shore hardness and flexural strength, which could effectively reduce the penetration depth and suppress the propagation of cracks, thus reducing the wear rate. However, the calcined

MCMB, only heat-treated at relative median temperature, had no remarkable lubrication effect to decrease the friction coefficient. Lots of debris with carbon and epoxy particles were peeled off from the surface, forming rough MML film. Meanwhile, the counterpart ball was only coated with some composite debris, unable to form lubricated layer to layer contact films. These factors can explain the high and unstable friction coefficient and reduced wear rate after adding CM filler. The wear was adhesive and abrasive wear.

E-g-AM/EP composite had adhesion and fatigue wear in this work. Besides having the influence from carbon spheres which can reduce the wear rate, it also had another two merits

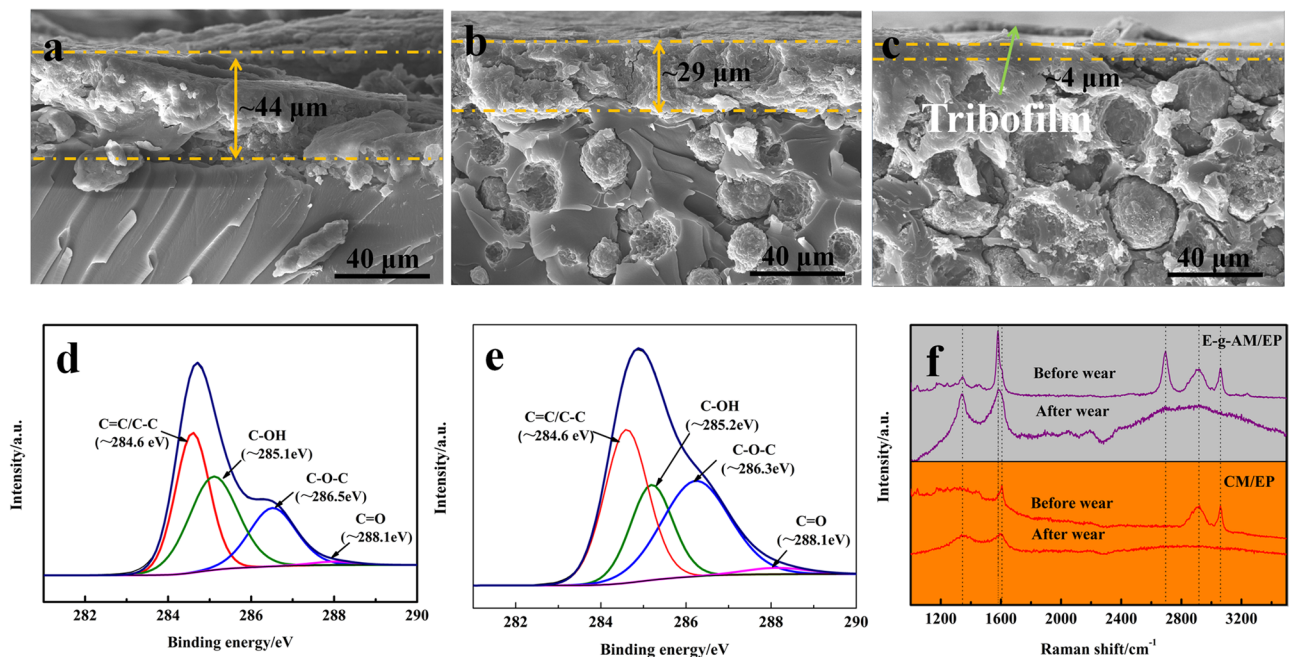


Fig. 11 **a–c** SEM images of longitudinal sections under worn scar of the three specimens: **a** neat epoxy; **b** 20%CM/EP; and **c** 20%E-g-AM/EP. XPS results of **d** E-g-AM/EP and **e** CM/EP. **f** Micro-Raman

spectroscopy of worn surfaces of 20%E-g-AM/EP and 20%CM/EP before and after wear test

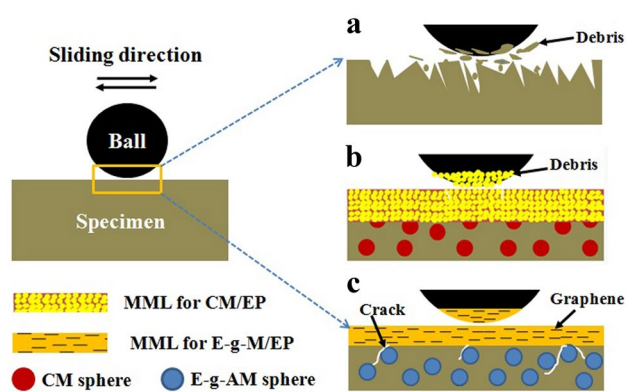


Fig. 12 Schematic diagram of the friction mechanism of the **a** neat EP; **b** CM/EP; and **c** E-g-AM

from graphene in E-g-AM/EP: strong interfacial bonding and well dispersed condition. The lubricating effect of graphene contributed to form thin and smooth MML, releasing the stress concentration. Moreover, the graphene would easily transfer onto the surface of counterpart ball, forming lubricated layer to layer contact. The two-dimensional planar geometry of graphene was beneficial to restrain crack propagation, thus regulating the debris size and reducing the wear rate [19]. But it is worth noting that strengthening the interface adhesion between graphene spheres and epoxy was very important, otherwise it can offer the path to crack propagation and worsen the fatigue wear. The improved heat dissipation capability also could enable to enhance the resistance of oxidation and decomposition of the composites.

5 Conclusion

g-AM spheres with excellent dispersion condition and facile preparation method were obtained in our previous work. In order to investigate the application potential as filler of polymer-based composite, three kinds of epoxy composites CM/EP, g-AM/EP, and E-g-AM/EP were prepared with simple method. Comparing with neat epoxy and CM/EP, the thermal and tribological properties of g-AM/EP were improved when the content was low. However, due to the weak interface interaction between graphene and epoxy, the above performance was decreased when the g-AM content was high. After chemical functionalization by grafting epoxy chain on the graphene, the total performance, especially the wear resistance, was remarkably improved even at high graphene content. The wear rate of E-g-AM/EP composite was reduced by 95% at 20% E-g-AM. This superior wear resistance was from the synergistic effect of carbon spheres and graphene. The carbon spheres improved shore hardness and flexural strength, thus reducing the wear rate. The

two-dimensional planar geometry of graphene was beneficial to restrain crack propagation and improve mechanical and thermal performance, reducing the wear rate. Strengthening the interface adhesion between graphene spheres and epoxy can further restrain crack propagation and improve the mechanical and thermal performance. The lubricating effect of graphene contributed to form thin and smooth MML with layer-to-layer contact, releasing the stress concentration.

Acknowledgements The authors are grateful to the Shaanxi Innovation Capacity Support Program (2018TD-031), Natural Science Foundation of Shaanxi (2018JQ5008), Fundamental Research Funds for the Central University (XJJ2018003), and Science and Technology project from Headquarters of State Grid Co., LTD (SGAH0000KJJS1900437).

Declarations

Conflict of interest The authors declare no competing interests.

References

- Rafiee R (2016) On the mechanical performance of glass-fiber-reinforced thermosetting-resin pipes: a review. *Compos Struct* 143:151–164. <https://doi.org/10.1016/j.compstruct.2016.02.037>
- Tang LC, Wan YJ, Yan D, Pei YB, Zhao L, Li YB, Wu LB, Jiang JX, Lai GQ (2013) The effect of graphene dispersion on the mechanical properties of graphene/epoxy composites. *Carbon* 60:16–27. <https://doi.org/10.1016/j.carbon.2013.03.050>
- Ahmad S, Gupta AP, Sharmin E, Alam M, Pandey SK (2005) Synthesis, characterization and development of high performance siloxane-modified epoxy paints. *Prog Org Coat* 54:248–255. <https://doi.org/10.1016/j.porgcoat.2005.06.013>
- Xavier JR (2020) Investigation on the anticorrosion, adhesion and mechanical performance of epoxy nanocomposite coatings containing epoxy-silane treated nano-MoO₃ on mild steel. *J Adhes Sci Technol* 34:115–134. <https://doi.org/10.1080/01694243.2019.1661658>
- Bustero I, Gaztelumendi I, Obieta I, Mendizabal MA, Zurutuza A, Ortega A, Alonso B (2020) Free-standing graphene films embedded in epoxy resin with enhanced thermal properties. *Adv Compos Hybrid Mater* 3(1):31–40. <https://doi.org/10.1007/s42114-020-00136-6>
- Zhang JX, Liang YX, Wang XJ, Zhou HJ, Li SY, Zhang J, Feng YN, Lu N, Wang Q, Guo ZH (2018) Strengthened epoxy resin with hyperbranched polyamine-ester anchored graphene oxide via novel phase transfer approach. *Adv Compos Hybrid Mater* 1(2):300–309. <https://doi.org/10.1007/s42114-017-0007-0>
- He Y, Wu D, Zhou M, Liu H, Zhang L, Chen Q, Yao B, Yao D, Jiang D, Liu C, Guo Z (2020) Effect of MoO₃/carbon nanotubes on friction and wear performance of glass fabric-reinforced epoxy composites under dry sliding. *Appl Surf Sci* 506:144946. <https://doi.org/10.1016/j.apsusc.2019.144946>
- Österle W, Dmitriev AI, Gradt T, Häusler I, Hammouri B, Morales Guzman PI, Wetzel B, Yigit D, Zhang G (2015) Exploring the beneficial role of tribofilms formed from an epoxy-based hybrid nanocomposite. *Tribol Int* 88:126–134. <https://doi.org/10.1016/j.triboint.2015.03.006>
- EL-Tayeb NSM, Liew KW (2009) On the dry and wet sliding performance of potentially new frictional brake pad materials for automotive industry. *Wear* 266:275–287. <https://doi.org/10.1016/j.wear.2008.07.003>

10. Shen XJ, Pei XQ, Fu SY, Friedrich K (2013) Significantly modified tribological performance of epoxy nanocomposites at very low graphene oxide content. *Polymer* 54:1234–1242. <https://doi.org/10.1016/j.polymer.2012.12.064>
11. Shen XJ, Pei XQ, Liu Y, Fu SY (2014) Tribological performance of carbon nanotube–graphene oxide hybrid/ epoxy composites. *Compos B Eng* 57:120–125. <https://doi.org/10.1016/j.compositesb.2013.09.050>
12. Lahiri D, Hec F, Thiesse M, Durygin A, Zhang C, Agarwal A (2014) Nanotribological behavior of graphene nanoplatelet reinforced ultra high molecular weight polyethylene composites. *Tribol Int* 70:165–169. <https://doi.org/10.1016/j.triboint.2013.10.012>
13. Wang H, Xie GY, Zhu ZG, Ying Z, Zeng Y (2014) Enhanced tribological performance of the multi-layer graphene filled poly(vinyl chloride) composites. *Compos Part A Appl Sci Manuf* 67:268–273. <https://doi.org/10.1016/j.compositesa.2014.09.011>
14. Zhao F, Zhang L, Li G, Guo Y, Qi H, Zhang G (2018) Significantly enhancing tribological performance of epoxy by filling with ionic liquid functionalized graphene oxide. *Carbon* 136:309–319. <https://doi.org/10.1016/j.carbon.2018.05.002>
15. Tai ZX, Chen YF, An YF, Yan XB, Xue QJ (2012) Tribological behavior of UHMWPE reinforced with graphene oxide nanosheets. *Tribol Lett* 46:55–63. <https://doi.org/10.1007/s11249-012-9919-6>
16. Wang TC, Xiong DS, Zhou T (2010) Preparation and wear behavior of carbon/epoxy resin composites with an interpenetrating network structure derived from natural sponge. *Carbon* 48:2435–2441. <https://doi.org/10.1016/j.carbon.2010.03.011>
17. Wetzela B, Hauptert F, Zhang MQ (2003) Epoxy nanocomposites with high mechanical and tribological performance. *Compos Sci Technol* 63:2055–2067. [https://doi.org/10.1016/S0266-3538\(03\)00115-5](https://doi.org/10.1016/S0266-3538(03)00115-5)
18. Mo Y, Yang ML, Lu ZX, Huang FC (2013) Preparation and tribological performance of chemically-modified reduced graphene oxide/polyacrylonitrile composites. *Compos Part A Appl Sci Manuf* 54:153–158. <https://doi.org/10.1016/j.compositesa.2013.07.014>
19. Kandannur SS, Rafiee MA, Yavari F, Schrameyer M, Yu ZZ, Blanchet TA, Koratkar N (2012) Suppression of wear in graphene polymer composites. *Carbon* 50:3178–3183. <https://doi.org/10.1016/j.carbon.2011.10.038>
20. Chen C, Qiu SH, Cui MJ, Qin SL, Yan GP, Zhao HC, Wang LP, Xue QJ (2017) Achieving high performance corrosion and wear resistant epoxy coatings via incorporation of noncovalent functionalized graphene. *Carbon* 114:356–366. <https://doi.org/10.1016/j.carbon.2016.12.044>
21. Min CY, Nie P, Song HJ, Zhang ZZ, Zhao KL (2014) Study of tribological properties of polyimide/graphene oxide nanocomposite films under seawater-lubricated condition. *Tribol Int* 80:131–140. <https://doi.org/10.1016/j.triboint.2014.06.022>
22. Yi M, Shen ZG (2015) A review on mechanical exfoliation for the scalable production of graphene. *J Mater Chem A* 3:11700–11715. <https://doi.org/10.1039/C5TA00252D>
23. Nicolosi V, Chhowalla M, Kanatzidis MG, Strano MS, Coleman JN (2013) Liquid exfoliation of layered materials. *Science* 340:1226419. <https://doi.org/10.1126/science.1226419>
24. Park SJ, Ruoff RS (2009) Chemical methods for the production of graphenes. *Nat Nanotechnol* 4:217–224. <https://doi.org/10.1038/nnano.2009.58>
25. Allen MJ, Tung VC, Kaner RB (2010) Honeycomb carbon: a review of graphene. *Chem Rev* 110:132–145. <https://doi.org/10.1021/cr900070d>
26. Viculis LM, Mack JJ, Kaner RB (2003) A chemical route to carbon nanoscrolls. *Science* 299:1361. <https://doi.org/10.1126/science.1078842>
27. Reina A, Jia XT, Ho J, Nezich D, Son H, Bulovic V, Dresselhaus SM, Kong J (2009) Large area, few-layer graphene films on arbitrary substrates by chemical vapor deposition. *Nano Lett* 9:30–35. <https://doi.org/10.1021/nl801827v>
28. Ryu J, Kim Y, Won D, Kim N, Park JS, Lee EK, Cho D, Cho SP, Kim SJ, Ryu GH, Shin HAS, Lee Z, Hong BH, Cho S (2014) Fast synthesis of high-performance graphene films by hydrogen-free rapid thermal chemical vapor deposition. *ACS Nano* 8:950–956. <https://doi.org/10.1021/nn405754d>
29. Kuila T, Bose S, Hong CE, Uddin ME, Khanra P, Kim NH, Lee JH (2011) Preparation of functionalized graphene/linear low density polyethylene composites by a solution mixing method. *Carbon* 49:1033–1037. <https://doi.org/10.1016/j.carbon.2010.10.031>
30. Potts JR, Lee SH, Alam TM, An J, Stoller MD, Piner RD, Ruoff RS (2011) Thermomechanical properties of chemically modified graphene/poly(methyl methacrylate) composites made by in situ polymerization. *Carbon* 49:2615–2623. <https://doi.org/10.1016/j.carbon.2011.02.023>
31. Wang JY, Yang SY, Huang YL, Tien HW, Chin WK, Ma CCM (2011) Preparation and properties of graphene oxide/polyimide composite films with low dielectric constant and ultrahigh strength via in situ polymerization. *J Mater Chem* 21:13569–13575. <https://doi.org/10.1039/C1JM11766A>
32. Xu X, Yang C, Yang J, Huang T, Zhang N, Wang Y, Zhou Z (2017) Excellent dielectric properties of poly(vinylidene fluoride) composites based on partially reduced graphene oxide. *Compos B Eng* 109:91–100. <https://doi.org/10.1016/j.compositesb.2016.10.056>
33. Wang P, Chong H, Zhang J, Yang Y, Lu H (2018) Ultralow electrical percolation in melt-compounded polymer composites based on chemically expanded graphite. *Compos Sci Technol* 158:147–155. <https://doi.org/10.1016/j.compscitech.2018.01.022>
34. Zaheer U, Khurram AA, Subhani T (2018) A treatise on multi-scale glass fiber epoxy matrix composites containing graphene nanoplatelets. *Adv Compos Hybrid Mater* 1(4):705–721. <https://doi.org/10.1007/s42114-018-0057-y>
35. Xia H, Wang K, Yang S, Shi Z, Wang H, Wang J (2016) Formation of graphene flowers during high temperature activation of mesocarbon microbeads with KOH. *Microporous Mesoporous Mater* 234:384–391. <https://doi.org/10.1016/j.micromeso.2016.07.046>
36. Shen B, Zhai W, Tao M, Lu D, Zheng W (2013) Chemical functionalization of graphene oxide toward the tailoring of the interface in polymer composites. *Compos Sci Technol* 77:87–94. <https://doi.org/10.1016/j.compscitech.2013.01.014>
37. Sadagopan K, Ratna D, Samui AB (2003) Synthesis and characterization of liquid-crystalline epoxy and its blend with conventional epoxy. *J Polym Sci Part A: Polym Chem* 41:3375–3383. <https://doi.org/10.1002/pola.10923>
38. Tang L, Zhang JL, Gu JW (2021) Random copolymer membrane coated PBO fibers with significantly improved interfacial adhesion for PBO fibers/cyanate ester composites. *Chinese J Aeronaut* 34(2):659–668. <https://doi.org/10.1016/j.cja.2020.03.007>
39. Xia HY, Wang JP, Shi ZQ, Liu GW, Qiao GJ (2012) Sliding wear behavior of mesocarbon microbeads based carbon materials. *Wear* 274–275:260–266. <https://doi.org/10.1016/j.wear.2011.09.004>
40. Xia HY, Qiao GJ, Zhou SL, Wang JP (2013) Reciprocating friction and wear behavior of reaction-formed SiC ceramic against bearing steel ball. *Wear* 303:276–285. <https://doi.org/10.1016/j.wear.2013.03.038>
41. Dhieb H, Buijnsters JG, Eddoumy F, Celis JP (2011) Surface damage of unidirectional carbon fiber reinforced epoxy composites under reciprocating sliding in ambient air. *Compos Sci Technol* 71:1769–1776. <https://doi.org/10.1016/j.compscitech.2011.08.012>